Folding of Tryptophan Mutants of Barstar: Evidence for an Initial Hydrophobic Collapse on the Folding Pathway†

Utpal Nath and Jayant B. Udgaonkar*

National Centre for Biological Sciences, TIFR Centre, P.O. Box 1234, Indian Institute of Science Campus, Bangalore 560012, India

Received February 25, 1997; Revised Manuscript Received May 8, 1997⊗

ABSTRACT: The contributions of the three tryptophan residues of barstar to the spectroscopic properties, stability, and folding of the protein have been studied by mutating two of the tryptophans, *Trp38* and *Trp44*, individually as well as together, to phenylalanines, *Phe*. The three mutant proteins studied are shown to be similar to *wt* barstar in structure by activity measurements as well as by spectroscopic characterization. Fluorescence energy transfer between the tryptophans as well as quenching by their local structural environments complicates the analysis of the contributions of the individual tryptophans to the fluorescence of the *wt* protein, but it is demonstrated that *Trp53*, which is completely buried within the hydrophobic core, makes the dominant contribution to the fluorescence, while the fluorescence of *Trp38* is largely quenched in the fully folded protein. GdnHCl- as well as temperature-induced equilibrium unfolding studies, using three different structural probes, indicate that *W38FW44F*, where both *Trp38* and *Trp44* have been removed, follows a two-state unfolding transition and is less stable than the *wt* barstar. The fluorescence-monitored folding and unfolding kinetics of *W38FW44F* have been studied in detail. *W38FW44F* folds 2-fold faster and unfolds 3-fold faster than *wt* barstar. A large fraction of the total fluorescence change that occurs during folding occurs in a burst phase within 4 ms after commencement of folding. A similar burst phase change in fluorescence, although to a smaller extent, is shown to occur during the folding of *wt* barstar. The results suggest that a very early folding intermediate accumulates within 4 ms of folding, and that this kinetic intermediate is sufficiently compact that *Trp53*, which is completely sequestered from solvent in the fully folded protein, is also significantly sequestered from solvent in this intermediate.

It has been recognized for a long time that proteins must fold along one or a few folding pathways (Levinthal, 1968). Only a few proteins are known to fold directly from the fully unfolded state to the fully folded state without the detectable accumulation of any intermediate on the folding pathway (Jackson *et al.*, 1993; Kragelund *et al.*, 1995; Schindler *et al.*, 1995). For the vast majority of proteins that have been studied, partly folded structural intermediates accumulate on, and define, the folding pathways [see reviews by Kim and Baldwin (1990), Matthews (1993), Nath and Udgaonkar (1997), and Roder and Colón (1997)]. Much structural information is now available on folding intermediates from the application of many physical techniques [reviewed by Plexco and Dobson (1996)] to study folding kinetics, as well as from the application of protein engineering methodologies [reviewed by Matouschek and Fersht (1991)].

A common feature of protein folding pathways, which has emerged from the structural characterization of the folding pathways of many proteins, is that they are populated by molten globule intermediates with partial secondary structure stabilized by minimal native-like tertiary interactions, if any. Recent studies have shown that molten globule intermediates, which were first characterized extensively as equilibrium intermediates (Kuwajima, 1989; Hughson *et al.*, 1990; Ptitsyn, 1992; Fink, 1995), do accumulate actually on kinetic folding pathways (Jennings & Wright, 1993; Arai & Kuwajima, 1996).

In general, molten globule intermediates accumulate early on the folding pathway, very often in a burst phase of a few milliseconds after commencement of folding (Jennings & Wright, 1993; Arai & Kuwajima, 1996). The extent of secondary structure developed in these intermediates can be monitored by rapid mixing circular dichroism (CD)[1] techniques (Kuwajima *et al.*, 1987) as well as by pulsed amide hydrogen exchange methods coupled with NMR [reviewed by Baldwin (1993)]. The clustering of hydrophobic residues in these intermediates is easily monitored by their ability to bind hydrophobic dyes such as ANS (Semisotnov *et al.*, 1991; Engelhard & Evans, 1995; Shastry & Udgaonkar, 1995). The locations of such clusters cannot, however, be determined directly; in particular, it is not known whether kinetic molten globules have solvent-accessible hydrophobic cores (Ptitsyn, 1992). Moreover, while it is known that equilibrium molten globules are compact, the degree of compactness in kinetic molten globules can only be inferred from their equilibrium counterparts because direct methods for measuring compactness with millisecond time resolution

† This work was funded by the Tata Institute of Fundamental Research and by the Department of Biotechnology, Government of India.

* Corresponding author. Fax: 91-80-3343851. E-mail:jayant@ncbs.tifrbng.res.in.

⊗ Abstract published in *Advance ACS Abstracts,* June 15, 1997.

[1] Abbreviations: *W38F*, *Trp38→Phe* mutant form of barstar; *W44F*, *Trp44→Phe* mutant form of barstar; *W38FW44F*, a *Trp38→Phe*, *Trp44→Phe* double mutant form of barstar; GdnHCl, guanidine hydrochloride; CD, circular dichroism; DTT, dithiothreitol; ANS, 8-anilino-1-naphthalenesulfonic acid.

S0006-2960(97)00426-1 CCC: $14.00

do not exist (Eliezer *et al*., 1995). Obtaining detailed information on the degree of development of side chain−side chain interactions as well as on the development of the hydrophobic core in molten globule intermediates is a major goal of current studies in protein folding.

Barstar, a small bacterial ribonuclease inhibitor, is an excellent model protein for folding studies. A very good expression system in *Escherichia coli* is available (Hartley, 1988). Both crystal (Guillet *et al*., 1993) and solution structures (Lubienski *et al*., 1994) are known to high resolution. Barstar undergoes completely reversible unfolding transitions whether denatured by urea, GdnHCl, temperature, high pH, or low pH (Khurana & Udgaonkar, 1994). At low pH, it exists in a molten globule-like form (Khurana & Udgaonkar, 1994; Swaminathan *et al*., 1994). Extensive folding (Schreiber & Fersht, 1993; Shastry *et al*., 1994; Shastry & Udgaonkar, 1995; Agashe *et al*. 1995; Nölting *et al*., 1997) and unfolding (Nath *et al*., 1996) kinetic studies have already been used to characterize the folding and unfolding pathways of barstar.

Fluorescence-monitored folding and unfolding experiments (Schreiber & Fersht, 1993; Shastry *et al*., 1994) demonstrated that the fully folded protein, F, unfolds to an unfolded form, U_F, which can refold rapidly. U_F then undergoes a slow conformational transition, accompanied presumably by *cis* to *trans* isomerization of the *Tyr47*−*Pro48* peptide bond (Schreiber & Fersht, 1993), to another unfolded form, U_S, which can refold only much slower. Equilibrium-unfolded barstar comprises of 69% U_S and 31% U_F molecules.

The major folding pathway of barstar has been shown (Shastry & Udgaonkar, 1995) to be

$$U_S \rightarrow I_{M1} \rightarrow I_{S1} \rightarrow I_N \rightarrow F$$

I_{M1} is a pre-molten globule intermediate devoid of any optically active secondary structure (Agashe *et al*., 1995), but nevertheless compact. I_{S1} is a molten globule intermediate with partial secondary structure, and I_N is a late native-like intermediate capable, like the fully folded protein, F, of inhibiting barnase (Schreiber & Fersht, 1993). While all three intermediates possess solvent-exposed hydrophobic clusters by virtue of their ability to bind ANS (Shastry & Udgaonkar, 1995), it is not known whether they, and I_{M1} in particular, are sufficiently compact so as to exclude water from their hydrophobic cores.

Barstar has three tryptophan residues at positions 38, 44, and 53 (Figure 1). To understand the contributions of these *Trp* residues to the spectroscopic properties, folding, and stability of barstar, and to monitor the folding kinetics of the core of the protein, the three tryptophans were mutated to phenylalanines. The three *Trp* residues were mutated one or two at a time to generate mutant proteins containing two (*viz*., *W38F*, *W44F*, and *W53F*) or one (*viz*., *W38FW44F*, *W44FW53F*, and *W38FW53F*) *Trp* residues. The mutant proteins *W38F*, *W44F*, and *W38FW44F* have been studied in detail. The other three mutant proteins, in which *Trp53* was mutated, could not be studied because of extremely low expression levels.

Here, it is shown that replacement of either *Trp38* or *Trp44* or both with *Phe* does not significantly alter the structure or activity of barstar. The contributions of the three *Trp* residues to the fluorescence properties of barstar have been studied, and it is shown that the major contribution to the fluorescence comes from *Trp53* and that the fluorescence of *Trp38* remains fully quenched in the native protein. The fluorescence-monitored folding and unfolding kinetics of *W38FW44F* (which contains only *Trp53*) have been studied in detail. Our data suggest that the folding kinetics of the mutant are altered significantly from those of the *wt*, by the replacement of the two partially buried *Trp* residues by *Phe* residues in the former. It is shown that while *W38FW44F* is less stable than *wt* barstar, its observable rate of folding as well as rate of unfolding is significantly faster than that of the *wt* protein. The burst phase intermediate I_{M1} is sufficiently compact so that *Trp53*, which is completely buried in the hydrophobic core of F, is not hydrated in I_{M1}.

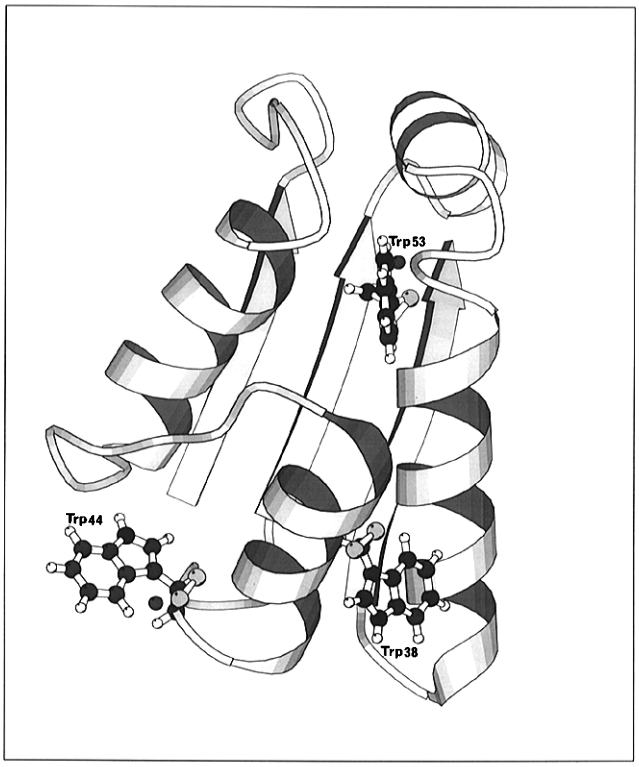

FIGURE 1: Solution structure of barstar (Lubienski *et al*., 1994) showing the locations of three tryptophan residues. *Trp38* is in the middle of helix 2 (residues 33−44), *Trp44* is at the end of helix 2, and *Trp53* is on the second strand of the β-sheet (residues 50−55) and resides in the hydrophobic core of the protein (Lubienski *et al*., 1994). *Trp53* is fully (99%) buried in the core of the protein where it makes close hydrophobic contacts with *Ile5*, *Leu16*, *Leu51*, *Phe56*, *Ala67*, *Val70*, and *Leu71*. *Trp44* is 40% buried and is in close hydrophobic contacts with *Leu26*, *Pro27*, *Cys40*, and *Val45*. *Trp38* is 70% buried and is in a negatively-charged environment created by *Glu76* and *Glu80*. The average distance between *Trp38* and *Trp44* is 14 Å, that between *Trp44* and *Trp53* is 19.3 Å, and that between *Trp38* and *Trp53* is 15.5 Å.

MATERIALS AND METHODS

Chemicals. GdnHCl, GpG, Yeast Torula RNA, and chromatographic resins were obtained from Sigma. SP-Trisacryl was purchased from IBF, and dialysis tubes of M_r 3500 cutoff, from Spectrum Medical Industries. Taq polymerase was from Boehringer Mannheim, and restriction enzymes were from New England Biolab. DNA sequencing was done using Sequenase version 2.0 obtained from Amersham. All other chemicals were of analytical grade.

Bacterial Strains, Plasmids, and Site-Directed Mutagenesis. The barnase and barstar expression plasmids, pMT416 and pMT316, respectively, were kindly provided by R. W. Hartley (1988). Oligonucleotide-directed mutagenesis was

done by PCR (Merino *et al*., 1992) on the plasmid pMT316, the barstar expression plasmid, as described earlier (Nath & Udgaonkar, 1995). The mutations were verified by dideoxy sequencing (Sanger *et al*., 1977) of the entire mutant barstar gene.

Expression and Purification of Barstar and Barnase. The procedure for the purification of the *W38F*, *W44F*, and *W38FW44F* mutant proteins was similar to that described earlier for *wt* barstar (Khurana & Udgaonkar, 1994). The yields of these proteins were 50−80% of that of *wt* barstar, which is ∼ 200 mg/L of cell growth. Barnase was purified as described by Mossakowska *et al*. (1989); the yield obtained was ∼8 mg/L.

Protein Concentration. Protein concentrations were estimated by a colorimetric method (Bradford, 1976). Extinction coefficients were determined by measuring the absorption at 280 nm of protein solutions of known concentrations. For subsequent experiments, ϵ_{280} values were used to determine the protein concentrations.

Inhibition Assay for Barstar Using GpG as the Substrate. The ability of the mutant proteins, in comparison to that of *wt* barstar, to inhibit the barnase-catalyzed hydrolysis of GpG was determined as previously described (Mossakowska *et al*., 1989; Nath & Udgaonkar, 1995).

Data Collection. All spectra were collected in 20 mM sodium phosphate, 0.5 mM EDTA, and 0.2 mM DTT, at pH 7.0 and 25 °C. All buffers used were of the highest purity grade. For all experiments, solutions were passed through 0.22 μm filters and degassed before use.

Absorption spectra were collected on a Cary 1 spectrophotometer thermostated by a Cary Peltier device using a cuvette of 1 cm path length. All spectra were the average of at least 3 scans. The protein concentration in the cuvette was typically 0.1−0.2 mg/mL.

Fluorescence spectra were collected on a Spex fluorometer. The excitation wavelength and slit width were set at 295 nm and 0.1 mm, respectively, and emission was monitored from 300 to 400 nm with the emission slit width set at 4 mm. Each spectrum was the average of at least 15 scans, each with a time resolution of 2 s. The protein concentration in the cuvette was typically 2 μM, and the path length of the cuvette used was 1 cm.

CD spectra were collected on a Jasco 720 spectropolarimeter with a bandwidth of 1.0 nm, response time of 1 s, and scan speed of 20 nm/min. Each spectrum was the average of at least 20 scans. Cuvettes of path length 0.1 and 1 cm were used for far-UV and near-UV CD, respectively, and the protein concentration used was ∼20 and ∼75 μM, respectively.

Equilibrium Unfolding Studies. Equilibrium unfolding as a function of GdnHCl concentration was monitored by far-UV CD, near-UV CD, and fluorescence. The concentration of the GdnHCl stock solution was estimated from its refractive index (Pace *et al*., 1989). In each case, the protein was equilibrated for at least 4 h prior to the measurement. Incubation for 20 h gave similar results. All experiments were done at 25 °C.

Far-UV CD measurements were made using a protein concentration of 20 μM and a cuvette of path length 0.1 cm, while near-UV CD measurements were made using a protein concentration of 50 μM and a cuvette of path length 1 cm. For fluorescence-monitored melts, the excitation wavelength was 295 nm (slit width = 0.1 mm), and emission was monitored at the λ_{max} (emission) using an emission slit width of 4 nm. Measurements were made using ∼2 μM protein in a 1.0 cm path length cuvette.

Thermal Denaturation. Thermal denaturations were done in 20 mM sodium phosphate, 200 μM DTT, and 250 μM EDTA buffer at pH 7.0. Denaturation was followed by monitoring mean residue ellipticities at 220 (far-UV) and 275 nm (near-UV) using the Jasco J720 spectropolarimeter and a Neslab RTE-110 circulating bath. A cylindrical cuvette of 1 cm path length was used, and the samples were layered with mineral oil to avoid evaporation of sample during the experiment. No sample evaporation could be detected after the experiment. Temperature was monitored directly in the cuvette by a Thermolyne temperature probe. The accuracy of the probe was ±0.5 °C. Sufficient time was allowed after each raise of temperature for the sample to equilibrate.

Kinetic Experiments. All the kinetic experiments were carried out in a buffer containing 20 mM sodium phosphate, 0.5 mM EDTA, and 0.5 mM DTT at pH 7.0, 25 °C (native buffer). Rapid mixing was carried out in a Biologic SFM-3 stopped-flow machine as described previously (Shastry *et al.*, 1994). For folding experiments, barstar was unfolded in buffer containing 6 M GdnHCl for at least 2 h prior to the measurement, and folding was initiated by a 2−10-fold dilution of the protein solution. For unfolding experiments, protein in native buffer was diluted with different proportions of native and unfolding buffers (native buffer + 7.2 M GdnHCl) to obtain different final concentrations of GdnHCl. The path length of the cuvette used was 1.5 mm, and protein concentrations ranged from 10 to 50 μM.

Data Analysis. Raw equilibrium denaturation data were converted to plots of f_{app} versus denaturant concentration using the equation:

$$f_{app} = \frac{Y_o - (Y_F + m_F[D])}{(Y_U + m_U[D]) - (Y_F + m_F[D])} \quad (1)$$

Y_O is the observed signal at a particular GdnHCl concentration. Y_F and Y_U represent the intercepts, and m_F and m_U are the slopes of the native and the unfolded baselines, respectively, and were obtained by extrapolation of linear least-squares fits of the baselines.

To determine whether the application of a two-state F ⇌ U unfolding model was appropriate for analyzing the GdnHCl-induced denaturation data, f_{app} values were fit to

$$f_{app} = \frac{\exp[-(\Delta G_U + m_G[D])/RT]}{1 + \exp[-(\Delta G_U + m_G[D])/RT]} \quad (2)$$

In eq 2, f_{app} is related to ΔG_U by a transformation of the Gibbs−Helmholtz equation in which the equilibrium constant for unfolding in the folding transition zone, K_{app}, is given by $K_{app} = f_{app}/(1 - f_{app})$, for a two-state transition. It is also implicit in eq 2 that the free energy of unfolding is dependent linearly on denaturant concentration (Agashe & Udgaonkar, 1995):

$$\Delta G_U = \Delta G_U(H_2O) + m_G[D] \quad (3)$$

For the two-state F ⇌ U model, the midpoint of the equilibrium unfolding curve, C_m, which is the concentration of GdnHCl where the protein is half-unfolded, is given by $C_m = -\Delta G_U(H_2O)/m_G$.

The observable folding kinetics in the pretransition region were described by a 2-exponential process (Shastry *et al*.,

Table 1: Activities and Spectroscopic Characterization of the *Trp* Mutant Proteins

				fluorescence[c]					
		UV absorbance[b]		−GdnHCl		+6 M GdnHCl		mean residue ellipticity[d]	
protein	relative activity[a]	$\Delta\epsilon_{287}$	$\Delta\epsilon_{292}$	λ_{max}	F_{max}	λ_{max}	F_{max}	θ_{222}	θ_{275}
wt barstar	1.00	1820	910	334	1.00	356	0.74	-14700	-205
W38F	0.88	1260	1100	329	0.98	356	0.46	-14350	-150
W44F	0.87	1650	1070	332	0.77	356	0.44	-15280	-170
W38FW44F	0.99	1580	1440	327	0.88	356	0.23	-14400	-160

[a] All activities are relative to a value of 1 for *wt* barstar. [b] In M^{-1} cm^{-1}. [c] All fluorescence intensities are relative to a value of 1 for *wt* barstar in the absence of GdnHCl. [d] In deg cm^2 $dmol^{-1}$.

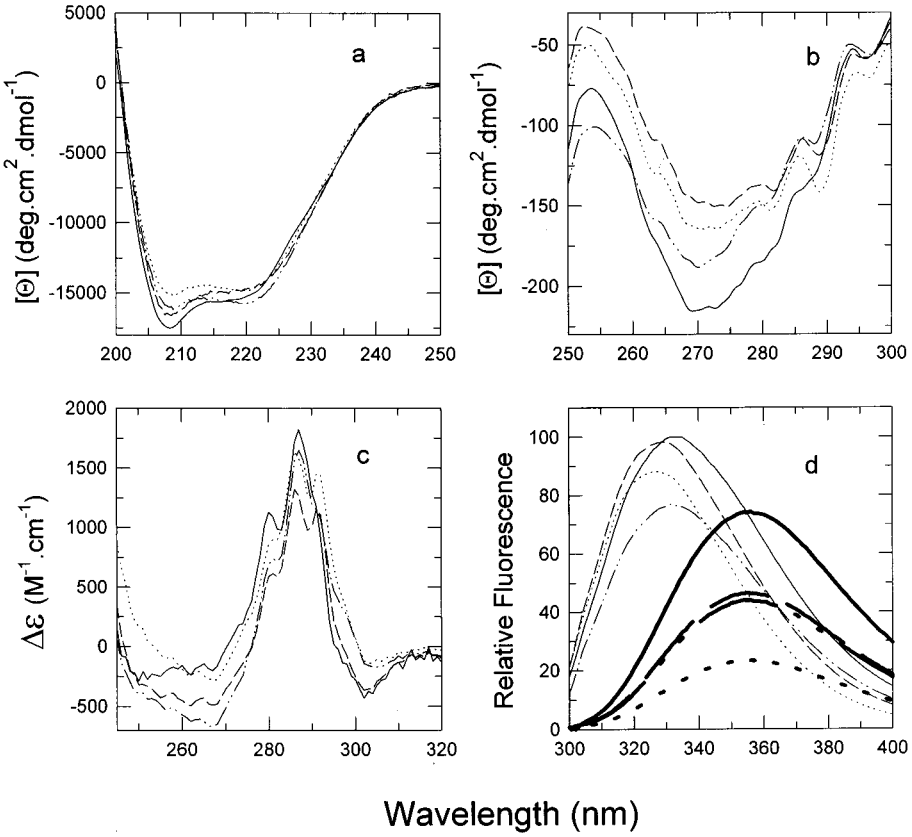

FIGURE 2: Spectroscopic characterization of *wt* barstar (—), *W38F* (− −), *W44F* (− · −), and *W38FW44F* (···) at pH 7, 25 °C. (a) Dependence of mean residue ellipticity on wavelength in the peptide region. (b) Dependence of mean residue ellipticity on wavelength in the aromatic region. (c) Difference UV absorption spectra. The difference in molar extinction coefficients of the proteins in the absence and presence of 6.0 M GdnHCl is plotted against wavelength. Unfolding of *wt* barstar is accompained by a value for $\Delta\epsilon_{281}$ of 1090 M^{-1} cm^{-1}, unfolding of *W38F* is accompanied by a value for $\Delta\epsilon_{281}$ of 615 M^{-1} cm^{-1}, unfolding of *W44F* is accompanied by a value for $\Delta\epsilon_{281}$ of 740 M^{-1} cm^{-1}, and unfolding of *W38FW44F* is accompanied by a value for $\Delta\epsilon_{281}$ of 900 $M^{-1}cm^{-1}$. (d) Fluorescence emission spectra of *wt* barstar and the *Trp* mutant proteins in the absence (thin lines) and in the presence (thick lines) of 6.0 M GdnHCl, on excitation at 295 nm. The values of the maximum fluorescence intensities and λ_{max} are shown in Table 1.

1994):

$$F(t) = F(\infty) - F_1 \exp(-\lambda_1 t) - F_2 \exp(-\lambda_2 t) \quad (4)$$

Unfolding kinetics in the transition region were also described by a 2-exponential process:

$$F(t) = F(\infty) + F_1 \exp(-\lambda_1 t) + F_2 \exp(-\lambda_2 t) \quad (5)$$

where λ_1 and λ_2 are the apparent rate constants of the slow and fast phases, and F_1 and F_2 are the respective amplitudes. The relative amplitudes of the slow and fast phases, α_1 and α_2, respectively, were determined by dividing the amplitude of the corresponding observed slow and fast phases by the equilibrium amplitude of the reaction at that GdnHCl concentration.

Unfolding kinetics in the posttransition region were described by a single exponential process: eq 5 was used with F_1 set to zero.

The dependence of λ_2 on GdnHCl concentration, in either the pretransition region or the posttransition region, is given by the equation (Tanford, 1970):

$$\ln \lambda_2 = \ln \lambda_2(H_2O) + m_{\lambda 2}[D] \quad (6)$$

where $\lambda_2(H_2O)$ is the rate constant of the fast phase when the protein is either unfolded or refolded in water.

RESULTS

Structures and Activities of the Trp Mutant Proteins. Table 1 and Figure 2 compare the spectroscopic properties and activities of the *Trp* mutant proteins with those of *wt* barstar. *W38F*, *W44F*, and *W38FW44F* retain 88%, 87%, and 99% of the barnase-inhibiting activity of *wt* barstar, respectively (Table 1). The far-UV CD spectra of the mutant proteins are similar to that of the *wt* protein (Figure 2a), as

are the values of the mean residue ellipticity at 222 nm, which is a measure of the helicity of a protein (Table 1). Figure 2b compares the near-UV CD spectra, which measure the asymmetric environments of the aromatic residues, of the four proteins. The mean residue ellipticity at 275 nm of each of the mutant proteins is significantly less (-160 ± 20) than in the *wt* barstar (-205 ± 20) (Table 1).

The extinction coefficients of *wt* barstar, *W38F*, *W44F*, and *W38FW44F* at 280 nm are 23 000, 15 500, 15 000, and 10 000 M^{-1} cm^{-1}, respectively. The value of ϵ_{280} for *wt* barstar reported here is the same as reported earlier (Khurana & Udgaonkar, 1994).

Figure 2c demonstrates that the UV absorption difference spectra, which measure the differences in the environments of the aromatic groups in the folded and unfolded states, of *W38F*, *W44F*, and *W38FW44F* are similar to that of *wt* barstar. As reported earlier (Khurana & Udgaonkar, 1994), such a spectrum for *wt* barstar exhibits peaks at 280 and 287 nm with a shoulder at 292 nm. In the cases of *W38F* and *W38FW44F*, distinct peaks are seen at 292 nm. The changes in the values of the extinction coefficients at 287 and 292 nm, $\Delta\epsilon_{287}$ and $\Delta\epsilon_{292}$, respectively, are shown in Table 1.

Fluorescence Properties of the Trp Mutant Proteins. Fluorescence emission spectra of the native and unfolded mutant and *wt* proteins are presented in Figure 2d. The spectra of the three mutant proteins show blue-shifts to different extents. The wavelength of maximum emission (λ_{max}) is decreased by 5 nm by removal of only *Trp38* (in *W38F*), by 2 nm by removal of only *Trp44* (in *W44F*), and by 7 nm by removal of both *Trp38* and *Trp44* (in *W38FW44F*) (Table 1). Removal of only *Trp38* (in *W38F*) does not alter the maximum fluorescence intensity, while removal of only *Trp44* (in *W44F*) decreases the maximum fluorescence intensity by 23%. Removal of both *Trp44* and *Trp38* (in *W38FW44F*) results in a decrease in the maximum fluorescence intensity by only 12% (Table 1). Under unfolding conditions (6 M GdnHCl), the λ_{max} for emission is 356 nm for each protein. The maximum fluorescence intensities of the four unfolded proteins at 356 nm are as expected from the number of tryptophan residues present in them (Table 1).

GdnHCl-Induced Denaturation Curves. In Figure 3 are shown GdnHCl-induced denaturation curves of *wt* (Figure 3a) barstar and *W38FW44F* (Figure 3b) monitored by two probes of tertiary structure, fluorescence intensity and near-UV CD, and one probe of secondary structure, far-UV CD. All three probes yield a value for C_m of 1.95 ± 0.05 in the case of *wt* barstar, and a value of 1.75 ± 0.05 M in the case of *W38FW44F* (for each protein, the value is the average of three repetitions using each probe). The value obtained for C_m for *wt* barstar is similar to that reported earlier (Khurana & Udgaonkar, 1994; Shastry *et al*., 1994).

GdnHCl-induced equilibrium unfolding curves were also obtained for *W38F* and *W44F* (data not shown). In the case of *W38F*, the fluorescence-monitored as well as the far-UV CD-monitored unfolding curves yield a value of 1.89 ± 0.05 M for C_m, while the near-UV CD-monitored unfolding curve yields a lower value for C_m, 1.73 ± 0.05 M. Similarly, in the case of *W44F*, the fluorescence and far-UV CD-monitored value of C_m is 1.87 ± 0.05 M, and the near-UV CD-monitored value is 1.77 ± 0.01 M. The errors in the values of C_m represent the standard deviations based on at least three repetitions using each probe, and the small differences in the values obtained using different optical probes are therefore significant, and suggest that equilibrium unfolding intermediates accumulate in the folding of *W38F* and *W44F*.

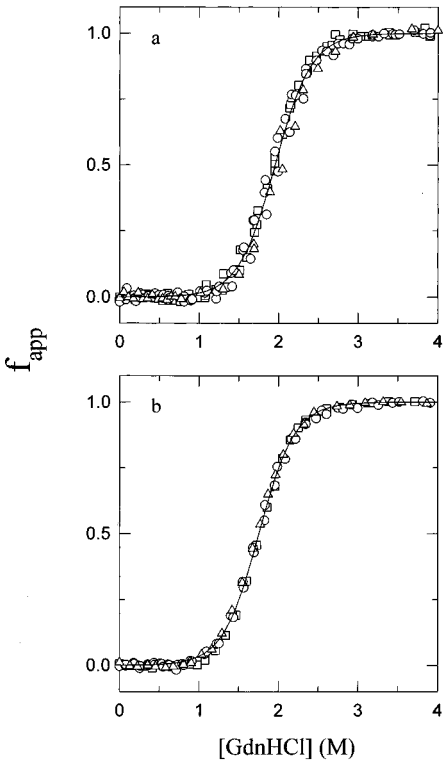

FIGURE 3: Equilibrium denaturation curves of *wt* barstar (a) and *W38FW44F* (b) at 25 °C, pH 7. GdnHCl-induced unfolding was followed by monitoring the mean residue ellipticity at 220 nm (○), the mean residue ellipticity at 275 nm (△), and the intrinsic tryptophan fluorescence (□). Fluorescence was excited at 295 nm, and was measured at 334 nm for *wt* barstar and at 327 nm for *W38FW44F*. Raw data were converted to f_{app} values using eq 1, and are plotted against GdnHCl concentration. The solid lines through the data are nonlinear least-squares fits of the data to eq 2, and yielded values for ΔG_U and m_G of 5.0 kcal/mol and -2.6 kcal/(mol·M) for *wt* barstar, and 4.4 kcal/mol and -2.5 kcal/(mol·M) for *W38FW44F*.

Thermal Denaturation. Thermal denaturation curves for *wt* barstar and the three tryptophan mutant proteins were obtained using far- and near-UV CD as probes to monitor unfolding (data not shown). For all four proteins, both probes yielded coincident denaturation curves. The values obtained for T_m, the midpoint of the transition, of *wt* barstar, *W38F*, *W44F*, and *W38FW44F* are 70.0 ± 0.5, 69.6 ± 0.5, 70.0 ± 0.5, and 68.0 ± 0.5 °C, respectively.

Folding Kinetics of W38FW44F. Figure 4 illustrates the time course of change in fluorescence during the folding of *W38FW44F* in 0.7 M and 1.4 M GdnHCl. An extrapolation of the kinetic folding curve to $t = 0$ does not yield the value of fluorescence expected for completely unfolded protein. In 0.7 M GdnHCl, ~45% of the fluorescence change occurs in a burst phase (phase 0), within the dead time of mixing (4 ms), while in 1.4 M GdnHCl, only ~25% of the fluorescence change is complete in the burst phase. In each concentration of GdnHCl shown, the remainder of the change in fluorescence occurs in two observable phases, a fast phase (phase 2) in the 100 ms to 1 s time domain, and a slow phase (phase 1) in the hundreds of seconds time domain. The unfolding of *W38FW44F* also occurs in three similar phases when measured using GdnHCl concentrations in the transi-

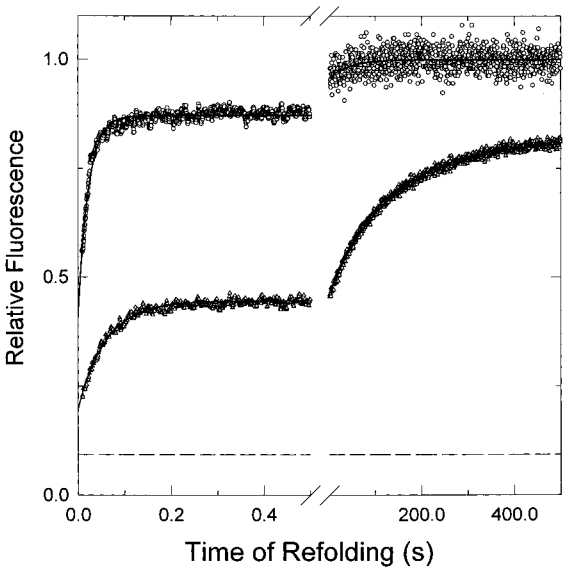

FIGURE 4: Kinetics of folding of *W38FW44F* at pH 7, 25 °C. Folding was carried out in 0.7 M GdnHCl (○) and 1.4 M GdnHCl (△). All fluorescence values were normalized to a value of 1 for protein in the absence of any GdnHCl. The lines through the data points represent nonlinear least-squares fits of the data to eq 4. The dashed line represents the fluorescence intensity of unfolded protein in 6 M GdnHCl.

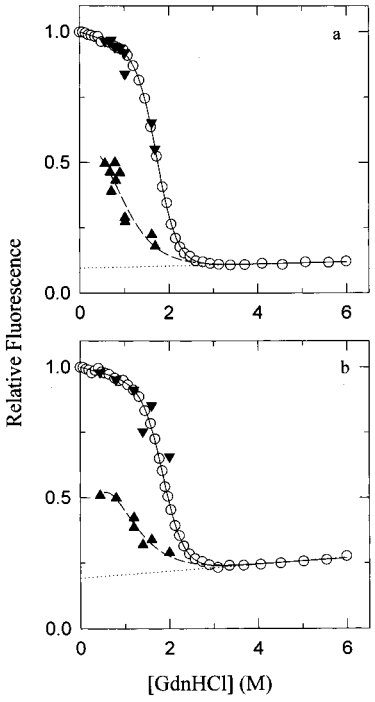

FIGURE 5: Kinetic and equilibrium amplitudes of folding of (a) *W38FW44F* and (b) *wt* barstar at pH 7, 25 °C. (○) Equilibrium unfolding curve; (▲) initial amplitude of the kinetic folding curve obtained by using eq 4 to extrapolate to $t = 0$; (▼), final amplitude of the kinetic folding curve obtained by using eq 4 to extrapolate to $t = \infty$. All amplitudes are relative to a value of 1 for F. The solid lines are fits of the equilibrium unfolding data to two-state F ⇌ U transitions (see Figure 3). The dotted lines are linear extrapolation of the unfolded protein base lines to low GdnHCl concentrations. The dashed lines have been drawn by inspection only.

tion zone, but is described by a single first-order process (phase 2) in the posttransition zone.

In Figure 5, the total observable kinetic amplitudes of folding of *W38FW44F* (Figure 5a) as well as of *wt* (Figure 5b) barstar are shown normalized to the amplitudes expected

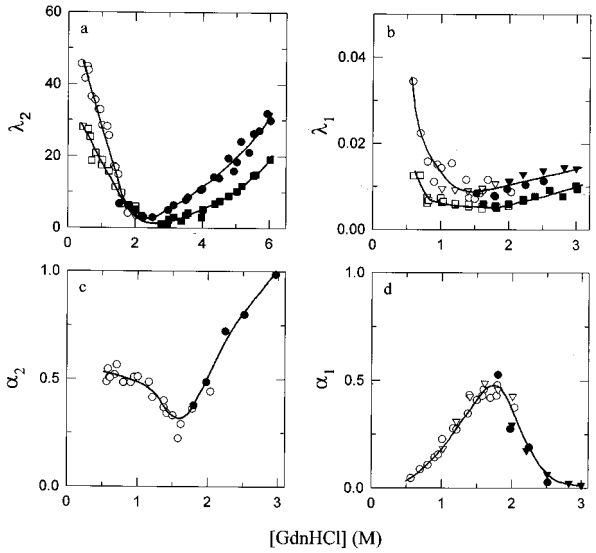

FIGURE 6: Apparent rate constants and relative amplitudes of the two observable kinetic phases in the folding of *W38FW44F* at pH 7, 25 °C. The dependencies of the apparent rate constants and relative amplitudes on the concentration of GdnHCl are shown. (○, ▽) Data obtained from folding experiments; (●, ▼) data obtained from unfolding experiments. Data obtained from manual mixing experiments are represented by (▽) and (▼), while those obtained from stopped-flow mixing experiments are represented by (○) and (●). Also shown for comparison are the rate constants for folding (□) and unfolding (■) of *wt* barstar. (a) Apparent rate constant of the fast phase, λ_2 . (b) Apparent rate constant of the slow phase, λ_1. (c) Relative amplitude of the fast phase, α_2. (d) Relative amplitude of the slow phase, α_1. All measurements had a standard deviation of ±10%. The solid lines have been drawn by inspection only.

from equilibrium unfolding curves, for concentrations of GdnHCl in the pretransition and transition zones. In each case, the total kinetic amplitude was obtained as $F_1 + F_2$ from a fit of the kinetic data to eq 4. As expected, the values obtained for F_∞ in each case fall on the equilibrium unfolding curve, indicating that the folding reactions have gone to completion. For concentrations of GdnHCl in the pretransition and transition zones, extrapolations of the kinetic folding curves to $t = 0$ do not, however, yield the fluorescence values expected for the fully unfolded protein, in the case of *wt* barstar as well as *W38FW44F*: the fluorescence values at $t = 0$ do not fall on the extrapolated unfolding baselines. Thus, the observed fast and slow phases of folding in a kinetic experiment do not account for the entire change in fluorescence seen in an equilibrium experiment for either protein. For the lowest concentration of GdnHCl used, 0.6 M, up to ~50% of the fluorescence change in the case of *W38FW44F* and up to ~35% in the case of *wt* barstar take place in a burst phase within 4 ms after the commencement of refolding. The burst phase change in fluorescence indicates the very rapid formation of an early intermediate on the folding pathway.

In Figure 6a,b, the dependencies on GdnHCl concentration of the apparent rate constants of the observed fast and slow kinetic phases, λ_2 and λ_1, respectively, are shown for the folding of *W38FW44F*. For comparison, data for *wt* barstar (Shastry *et al.*, 1994) are also shown. It is observed that the fast phase is at least 500-fold faster than the slow phase at all concentrations of GdnHCl used.

In Figure 6a, λ_2 in the case of *W38FW44F* is seen to decrease with increasing GdnHCl concentration up to a concentration of ~2.0 M, and then increase with a further

increase in GdnHCl concentration. Folding as well as unfolding experiments could be carried out for concentrations of GdnHCl between 1.5 and 2.0 M, and the values obtained for λ_2 from both types of experiments were the same. Thus, λ_2 depends on the final conditions and not on the initial conditions, as expected for a fully reversible folding reaction. The values of λ_2 in the pretransition zone were extrapolated to 0 GdnHCl concentration using eq 6 to obtain a value of 74 s^{-1} for λ_2 (folding) in water for *W38FW44F*. A similar extrapolation of the λ_2 values in the posttransition zone yields a value of 1.04 s^{-1} for λ_2 (unfolding) in water for *W38FW44F* (Nath *et al.*, 1996).

In Figure 6b, it is seen that λ_1 decreases marginally in value with increasing GdnHCl concentration in the pretransition zone, exhibits a broad minimum at ~1.4 M GdnHCl, and then increases marginally with a further increase in GdnHCl concentration. Again for concentrations of GdnHCl between 1.5 and 2.0 M, both folding and unfolding experiments gave identical values for λ_1. The values obtained for λ_1 using manual mixing experiments are the same as those obtained using stopped-flow mixing experiments.

In Figure 6c and Figure 6d are shown the GdnHCl dependencies of the fast observable change in fluorescence, α_2, and the slow observable change in fluorescence, α_1, when the folding of *W38FW44F* is carried out in concentrations of GdnHCl below 3 M. α_2 appears to decrease in value from 0.5 in 0.6 M GdnHCl to 0.3 in ~1.7 M GdnHCl, and then increases in value to 1.0 above ~3 M GdnHCl where only the fast phase in unfolding is observed. For concentrations of GdnHCl between 1.5 and 2.0 M, the value of α_2 does not depend on whether it was obtained from a folding or unfolding experiment. α_1 increases in value from 0.05 in 0.6 M GdnHCl to ~0.5 in 1.8 M GdnHCl, and then decreases in value to 0 in ~2.5 M GdnHCl. The dependence on GdnHCl concentration of α_1 for *W38FW44F* is very similar to that seen for *wt* barstar (Shastry *et al.*, 1994). For concentrations of GdnHCl between 1.5 and 2.0 M, α_1 has the same value regardless of whether it was obtained from a folding or unfolding experiment. The burst phase change in fluorescence, α_0, decreases in value from 0.5 in 0.6 M GdnHCl to 0 in ~2.5 M GdnHCl (Figure 5a).

DISCUSSION

Structures and Activities of the Trp Mutant Proteins. The barnase-inhibiting activities of the mutant proteins are unaltered by the mutations, indicating that the mutations do not affect the overall three-dimensional folds of the mutant proteins. Although both *Trp38* and *Trp44* take part in the barnase−barstar complex formation during inhibition (Guillet *et al.*, 1993; Buckle *et al.*, 1994), phenylalanine as a substituent in both cases could also establish similar contacts.

The mean residue ellipticities at 222 nm of the three mutant proteins are virtually the same as that of *wt* barstar, indicating that the helical content is not affected by the *Trp*→*Phe* substitutions (Figure 2a). Near-UV CD measures the asymmetric environments of aromatic residues. Tryptophan has more restriction in side-chain movement, because of its bulkier size, than phenylalanine and tyrosine. Thus, mutating *Trp38* or *Trp44* to *Phe* is expected to reduce the near-UV CD signal, as observed (Figure 2b). The observation that substitution of both *Trp38* and *Trp44* to *Phe* has the same effect on the near-UV CD signal as does substitution of either one of them is surprising, and suggests that the substitution of either *Trp* can significantly affect the asymmetry in the local environment of the other *Trp*, although the two *Trp* residues are well separated (Figure 1). The sharp negative peak at 288 nm originates probably from *Trp53* in *W38FW44F*. The difference UV absorption spectra of the mutant proteins (Figure 2c), compared to that of *wt* barstar, show that *Trp53* makes the predominant contribution to the change in absorption of barstar upon unfolding.

Fluorescence Properties of the Trp Residues in Barstar. It is difficult to predict the intrinsic fluorescence properties of a protein containing more than one tryptophan, even when the structure of the protein is known and when the fluorescence properties of single tryptophan-containing mutants are known, because they are complicated by local quenching and resonance energy transfer. The fluorescence intensity of a tryptophan residue can be quenched by neighboring side chains like free sulfhydryl, disulfide bonds, carboxyl groups, histidine (Loewenthal *et al*. 1991), methionine, *etc*. Resonance energy transfer (Wu & Brand, 1994) from one tryptophan to another in a protein can result in the donor residue being silent in fluorescence (Loewenthal *et al*., 1991).

The effects of removing either or both *Trp38* and *Trp44* on the λ_{max} and relative fluorescence intensity are shown in Table 1. In the folded state, the λ_{max} value of each of the three mutant proteins displays a blue shift with respect to the value for *wt* barstar. When both *Trp38* and *Trp44* are removed, the magnitude of the blue shift is equal to the sum of the magnitudes of the blue shifts seen when they are individually removed. The emission maximum of a tryptophan residue undergoes a blue shift when it gets buried in the hydrophobic environment of a protein. Since *Trp38* is less solvent-exposed than *Trp44* (Figure 1), removal of the former was expected to result in a smaller blue shift of the λ_{max} than removal of the latter, but the opposite result is seen (Table 1). Changes in fluorescence intensities are also difficult to interpret. Removal of only *Trp38* does not significantly affect the relative fluorescence intensity, because its fluorescence is probably quenched by the carboxyl groups of *Glu80* and *Glu76*, which are in close spatial proximity (Figure 1). Removal of *Trp44* reduces the fluorescence intensity by ~20%. The contribution of *Trp44* to the total fluorescence intensity is low because it is exposed partially to water, and, furthermore, its fluorescence may be partially quenched by *Cys40* (Ramachandran & Udgaonkar, 1996). *Trp*53, being fully buried in the hydrophobic core, contributes maximally to *wt* barstar fluorescence. Although *Trp*53 is next to *Glu52* in the sequence, its fluorescence cannot be quenched by *Glu52*, because these two residues are on the two opposite sides of the second β-strand. The fluorescence intensity of *W38FW44F* is slightly higher than that of *W44F*. This may be due to complex quenching behavior or to energy transfer from the completely buried *Trp53* to the partly buried *Trp38*. Under complete unfolding conditions, all of the proteins show fluorescence emission maxima at 356 nm, characteristic of tryptophans fully exposed to water (Table 1).

GdnHCl-Induced Unfolding. The observation that probes for secondary and tertiary structure yield coincident GdnHCl-induced denaturation curves for *wt* barstar and *W38FW44F* suggests that these two proteins unfold by a two-state F ⇌ U mechanism. It has, however, been demonstrated previously, by the use of fluorescence anisotropy measurements, that *W38FW44F* unfolds through a series of partly unfolded forms (Swaminathan *et al*., 1996). Thus, obtaining coinci-

dent denaturation curves using probes for secondary and tertiary structure does not prove that a two-state unfolding mechanism is operational. To obtain, however, an approximate measure of the stability of *W38FW44F*, a two-state mechanism was used to analyze its unfolding (see Results). Substitution of both *Trp38* and *Trp44* by *Phe*, in *W38FW44F*, causes marginal destabilization (Figure 3), probably because the smaller *Phe* cannot maintain the close hydrophobic interactions of *Trp38* with *Thr42*, *Val73*, and *Ala77*, or of *Trp44* with *Leu26*, *Pro27*, and *Cys40*. The lower stability of *W38FW44F* is observed in thermal denaturation also (T_m = 68 °C).

Refolding and Unfolding Kinetics of W38FW44F. The fluorescence-monitored kinetics of folding and unfolding of *W38FW44F* have been studied in detail because *W38FW44F* contains only *Trp53*, completely buried in the hydrophobic core. In this mutant protein, the fluorescence of *Trp53* reflects the degree to which it is hydrated. The kinetics of fluorescence change during folding are expected, therefore, to reflect the kinetics of sequestration of *Trp53* from water, presumably by a collapse of hydrophobic residues around it. For other proteins that possess unique *Trp* residues, fluorescence changes have been interpreted directly in terms of changes in their particular environments (Kiefhaber *et al.*, 1992; Varley *et al*., 1993; Khorasanizadeh *et al*., 1993, 1996). In proteins where the *Trp* is completely buried in the hydrophobic core (Khorasanizadeh *et al*., 1993, 1996), fluorescence intensity has been used to monitor directly the exclusion of water from the core as a result of its compaction during folding.

The fluorescence-monitored kinetics of folding of barstar in low concentrations of GdnHCl (Shastry *et al.*, 1994) as well as of urea (Schreiber & Fersht, 1993) have been characterized earlier. In both of these studies, it was reported that observable fast and slow phases in the folding kinetics account for essentially all (>90%) of the total fluorescence change during the folding of *wt* barstar (Schreiber & Fersht, 1993; Shastry *et al.*, 1994; Agashe *et al.*, 1995). In this study of the folding of *W38FW44F*, a substantial fraction (~50%) of the total change in fluorescence during folding in low concentrations of GdnHCl was observed to take place in an initial 4 ms burst phase (phase 0), with the fast (phase 2) and slow (phase 1) phases accounting for the remaining 50%. The burst phase change in the refolding of *wt* barstar was found to be ~35% in 0.6 M GdnHCl. In both of the earlier reports, the start and the end points of the kinetic traces had not been normalized to equilibrium denaturation curves, as done here for both *W38FW44F* and *wt* barstar in Figure 5. Instead, the amplitudes of the observable phases had been determined relative to the total change on complete folding of protein that had been unfolded in very high concentration of denaturant. The latter procedure leads to an underestimation of burst phase changes by approximately 10% at 0.6 M GdnHCl for *wt* barstar, because the unfolded protein baseline for *wt* barstar has a positive slope: the fluorescence of unfolded *wt* barstar increases with an increase in denaturant concentration (Figure 5b). In an earlier detailed study of the folding of *wt* barstar in 1.0 M GdnHCl (Agashe *et al*., 1995), ~12% burst phase change in intrinsic tryptophan fluorescence had been reported. If the slope of the unfolded protein base line had been taken into account, the burst phase change would have been determined instead to be ~22%, which is what is seen for folding in 1.0 M GdnHCl in Figure 5b.

Fast Phase of Folding (Phase 2). The fast rate constants of folding and unfolding of *W38FW44F* are significantly greater than those of *wt* barstar (Figure 6). The apparent refolding and unfolding rates in water are 74 and 1.0 s^{-1}, respectively, whereas the corresponding rates for *wt* barstar are 37 s^{-1} (Shastry *et al*., 1995) and 0.3 s^{-1} (Nath *et al*., 1996), respectively. Thus, *W38FW44F* refolds 2 times faster than *wt* barstar, but unfolds 3 times faster. The values of the equilibrium constants for unfolding in water, when determined as the ratios of the rate of unfolding in water to those of folding in water (1/74 for *W38FW44F*, 0.3/37 for *wt* barstar), do, as expected, indicate that *W38FW44F* is less stable than *wt* barstar (Figure 3). In general, there is no correlation between the stability of a protein and the rate of its folding. The marginally stable protein CspB folds extremely rapidly (Schindler *et al*., 1995). Similarly, the rates of folding for two fragments of the streptococcal G protein are inversely related with their stabilities (Alexander *et al*., 1992).

Slow Phase of Folding and Unfolding (Phase 1). Interestingly, the rate of the slow phase is also increased in *W38FW44F* by a factor of up to 3 as compared to the rate for *wt* barstar. The slow phase in barstar folding originates, at least in part, from the slow *trans*−*cis* isomerization of the *Tyr47*−*Pro48* peptide bond in the $I_N \rightarrow F$ step of the major folding pathway (Schreiber & Fersht, 1993; Shastry *et al*., 1995). *Trp38* and *Trp44* are nearer to *Pro48* than *Trp53*, and their fluorescence properties may be affected by the structural changes that take place in the $I_N \rightarrow F$ step of the major folding pathway to a greater extent than the fluorescence of *Trp53*.

Burst Phase of Folding (Phase 0). The earliest steps in protein folding are poorly understood. For most proteins, the formation of secondary structure cannot be resolved temporally from collapse of the polypeptide chain (Elöve *et al*., 1992; Radford *et al*., 1992; Chaffotte *et al*., 1992; Mann & Matthews, 1993). There are three possibilities (Nath & Udgaonkar, 1997): (1) secondary structure formation, at least in a nascent fluctuating form, precedes compaction of the polypeptide chain; (2) a nonspecific hydrophobic collapse precedes and facilitates subsequent secondary structure formation; and (3) secondary structure formation occurs concurrently with compaction of the polypeptide chain. In the case of barstar, both folding (Agashe *et al.*, 1995) and unfolding (Nath *et al.*, 1996) studies in GdnHCl have suggested that a nonspecific hydrophobic collapse precedes formation of any optically active secondary structure. The burst phase intermediate, I_{M1}, on the major folding pathway has been shown to be compact and devoid of secondary structure. The presence of a large burst phase (<4 ms) change in fluorescence of *Trp53* during the folding of *W38FW44F* indicates that water is expelled from the vicinity of *Trp53* in the initial step of folding to I_{M1}. Thus, I_{M1} must be sufficiently compact that *Trp53* has a greatly reduced solvent-accessibility. Hydrophobic clusters capable of binding ANS are known to be present in I_{M1} (Shastry & Udgaonkar, 1995), and the results reported here suggest that these solvent-accessible hydrophobic clusters might not be part of the hydrophobic cluster that forms initially to sequester *Trp53* from solvent.

Correlation to Protein Engineering Studies in the Microsecond Time Domain. In a recent study (Nölting *et al.*, 1997), the protein engineering approach (Matouschek *et al.*, 1990) has been used together with temperature-jump mea-

surements to characterize structure formation during the folding of barstar. In those measurements, a 0.2% change in total fluorescence, which accompanies the folding of 1% of molecules that are cold-denatured at 2 °C, was used to monitor folding in the submillisecond time domain after a temperature jump to 10 °C. The Φ value analysis in that study suggests that the hydrophobic residues that are in close contact with *Trp53* in the core (see legend to Figure 1) are as unstructured in the submillisecond intermediate (which corresponds to I_{M1}) as they are in the cold-denatured state. The only partial exception is *Leu16*, but that was expected anyway because it belongs to helix 1, which forms part of the residual structure seen in cold-denatured barstar (Wong *et al.*, 1996). This result of the protein engineering study, which reports only indirectly on structure formation, suggests that the core has not consolidated in I_{M1}. In contrast, if the hydrophobic collapse leading to very early sequestration of solvent from *Trp53* does indeed lead to the formation of a native-like hydrophobic core, then the results reported here would suggest that the core is consolidated to a substantial extent in I_{M1}.

In summary, this paper reports on the contributions of the individual *Trp* residues to the structure, stability and folding of barstar. It is shown that removing either *Trp38* or *Trp 44*, or both, affects these properties in unforeseen ways. *Trp53* makes the dominant contribution to the fluorescence properties of barstar. The major observation reported here is that the earliest observable intermediate, I_{M1}, forms as the result of a hydrophobic collapse in which *Trp53*, which is completely buried in the hydrophobic core of the fully folded protein, gets sequestered from water.

ACKNOWLEDGMENT

We thank M. K. Mathew for discussion, and for his comments on the manuscript.

REFERENCES

Agashe, V. R., & Udgaonkar, J. B. (1995) *Biochemistry 34*, 3286−3299.
Agashe, V. R., Shastry, M. C. R., & Udgaonkar, J. B. (1995) *Nature 377*, 754−757.
Alexander, P., Orban, J., & Bryan, P. (1992) *Biochemistry 31*, 7243−7248.
Arai, M., & Kuwajima, K. (1996) *Folding Des. 1*, 275−287.
Baldwin, R. L. (1993) *Curr. Opin. Struct. Biol. 3*, 84−91.
Bradford, M. M. (1976) *Anal. Biochem. 72*, 248−254.
Buckle, A. M., Schreiber, G., & Fersht, A. R. (1994) *Biochemistry 33*, 8878−8889.
Chaffotte, A. F., Cadieux, C., Guillou, Y., & Goldberg, M. E. (1992) *Biochemistry 31*, 4303−4308.
Eliezer, D., Jennings, P. A., Wright, P. E., Doniach, S., Hodgson, K. O., & Tsuruta, H. (1995) *Science 270*, 487−488.
Elöve, G. A., Chaffotte, A. F., Roder, H., & Goldberg, M. E. (1992) *Biochemistry 31*, 6876−6883.
Engelhard, M., & Evans, P. A. (1995) *Protein Sci. 4*, 1553−1562.
Fink, A. L. (1995) *Annu. Rev. Biophys. Biomol. Struct. 24*, 495−522.
Guillet, V., Lapthorn, A., Hartley, R. W., & Mauguen, Y. (1993) *Structure 1*, 165−176.
Hartley, R. W. (1988) *J. Mol. Biol. 202*, 913−915.
Hughson, F. M., Wright, P. E., & Baldwin, R. L. (1990) *Science 249*, 1544−1548.
Jackson, S. E., Elmasry, N., & Fersht, A. R. (1993) *Biochemistry 32*, 11270−11278.
Jennings, P. A., & Wright, P. E. (1993) *Science 262*, 892−895.
Khorasanizadeh, S., Peters, I. D., Butt, T. R., & Roder, H. (1993) *Biochemistry 32*, 7054−7063.
Khorasanizadeh, S., Peters, I. D., & Roder, H. (1996) *Nat. Struct. Biol. 3*, 193−205.
Khurana, R., & Udgaonkar, J. B. (1994) *Biochemistry 33*, 106−115.
Kiefhaber, T., Grunert, H. P., Hahn, U., & Schimd, F. X. (1992) *Proteins: Struct., Funct., Genet. 12*, 171−179.
Kim, P. S., & Baldwin, R. L. (1990) *Annu. Rev. Biochem. 59*, 631−660.
Kragelund, B. B., Robinson, C. V., Knudsen, J., & Dobson, C. M. (1995) *Biochemistry 34*, 7217−7224.
Kuwajima, K. (1989) *Proteins: Struct., Funct., Genet. 6*, 87−103.
Kuwajima, K., Yamaya, H., Miwa, S., Sugai, S., & Nagamura, T. (1987) *FEBS Lett. 221*, 115−118.
Levinthal, C. (1968) *J. Chem. Phys. 65*, 44.
Loewenthal, R., Sancho, J., & Fersht, A. R. (1991) *Biochemistry 30*, 6775−6779.
Lubienski, M. J., Bycroft, M., Freund, S. M. V., & Fersht, A. R. (1994) *Biochemistry 33*, 8866−8877.
Mann, C. J., & Matthews, C. R. (1993) *Biochemistry 32*, 5282−5290.
Matouschek, A., & Fersht, A. R. (1991) *Methods Enzymol. 202*, 82−112.
Matouschek, A., Kellis, J. T., Jr., Serrano, L., Bycroft, M., & Fersht, A. R. (1990) *Nature 346*, 440−445.
Matthews, C. R. (1993) *Annu. Rev. Biochem. 62*, 139−160.
Merino, E., Osuna, J., Bolivar, F., & Soberon, X. (1992) *BioTechniques 12*, 508−509.
Mossakowska, D. E., Nyberg, K., & Fersht, A. R. (1989) *Biochemistry 28*, 3843−3850.
Nath, U., & Udgaonkar, J. B. (1995) *Biochemistry 34*, 1702−1713.
Nath, U., & Udgaonkar, J. B. (1997) *Curr. Sci. 72*, 180−191.
Nath, U., Agashe, V. R., & Udgaonkar, J. B. (1996) *Nat. Struct. Biol. 3*, 920−923.
Nölting, B., Golbik, R., Neira, J. L., Soler-Gonzalez, A. S., Schreiber, G., & Fersht, A. R. (1997) *Proc. Natl. Acad. Sci. U.S.A. 94*, 826−830.
Pace, C. N., Shirley, B. A., & Thomson, J. A. (1989) in *Protein Structure: A Practical Approach* (Creighton, T. E., Ed.) pp 311−330, IRL Press, Oxford.
Plexco, K. W., & Dobson, C. M. (1996) *Curr. Opin. Struct. Biol. 6*, 630−636.
Ptitsyn, O. B. (1992) in *Protein Folding* (Creighton, T. E., Ed.) pp 243−300, WH Freeman & Co., New York.
Radford, S. E., Dobson, C. M., & Evans, P. A. (1992) *Nature 358*, 302−307.
Ramachandran, S., & Udgaonkar, J. B. (1996) *Biochemistry 35*, 8776−8785.
Roder, H., & Colón, W. (1997) *Curr. Opin. Struct. Biol. 7*, 1305−1322.
Sanger, F., Nicklen, S., & Coulson, A. R. (1977) *Proc. Natl. Acad. Sci. U.S.A. 74*, 5463−5467.
Schindler, T., Herrler, M., Mohamed, A., & Schmid, F. X. (1995) *Nat. Struct. Biol. 2*, 663−673.
Schreiber, G., & Fersht, A. R. (1993) *Biochemistry 32*, 11195−11203.
Semisotnov, G. V., Rodionova, N. A., Razgulyaev, O. I., Uversky, V. N., Gripas, A. F., & Golmanshin, R. I. (1991) *Biopolymers 31*, 119−128.
Shastry, M. C. R., & Udgaonkar, J. B. (1995) *J. Mol. Biol. 247*, 1013−1027.
Shastry, M. C. R., Agashe, V. R., & Udgaonkar, J. B. (1994) *Protein Sci. 3*, 1409−1417.
Swaminathan, R., Periasamy, N., Udgaonkar, J. B., & Krishnamoorthy, G. (1994) *J. Phys. Chem. 98*, 9270−9278.
Swaminathan, R., Nath, U., Udgaonkar, J. B., Periasamy, N., & Krishnamoorthy, G. (1996) *Biochemistry 35*, 9150−9157.
Tanford, C. (1970) *Adv. Protein Chem. 21*, 1−95.
Varley, P., Gronenborn, A. M., Christensen, H., Wingfield, P. T., Pain, R. H., & Clore, G. M. (1993) *Science 260*, 1110−1113.
Wong, K. B., Freund, S. M. V., & Fersht, A. R. (1996) *J. Mol. Biol. 259*, 805−818.
Wu, P., & Brand, L. (1994) *Anal. Biochem. 218*, 1−13.

BI970426Z